# Novel technique for measuring the 3D geometric size of fruit cells

Hongli Qiang[1], Baolong Li[1], Zhiguo Li[1*], Fideline Tchuenbou-Magaia[2], Boyuan Wei[3], Yande Liu[4]

(1. *College of Mechanical and Electronic Engineering, Northwest A & F University, Yangling 712100, Shaanxi, China*;
2. *Energy and green Technology Research Group, Centre for Engineering Innovation and Research, School of Engineering, Computing and Mathematical Sciences, University of Wolverhampton, Wolverhampton, WV1 1LY, UK*;
3. *Hazen Technology Co., Ltd, Ningbo, Zhejiang 315000, China*;
4. *Institute of Intelligent Electromechanical Equipment Innovation, East China Jiaotong University, Nanchang 330000, China*)

**Abstract:** The size and shape of individual fruit cells are key indicators of a fruit's physiological condition and overall quality. However, due to the three-dimensional (3D) nature of fruit cells, existing biomicroscopes are not capable of efficiently or accurately characterizing their 3D geometry. In this work, a novel microscope system integrated with computer software was developed to enable precise 3D geometrical characterization of fruit cells. To validate the system's effectiveness, tomatoes and strawberries at two different stages of ripeness were used as test samples. First, the front and bottom views of the fruit cells were captured. Subsequently, the developed software was used to measure the 3D geometric size of each individual cell. Key performance parameters of the developed 3D microscope, including overall magnification, aperture diameter, resolution, and field of view area, were carefully measured and evaluated. The experiment revealed differences in the length $D_1$, thickness $D_2$, width $D_3$, and geometric mean diameter ($GMD$) of single cells of tomatoes and strawberries; these differences were 18.18%, 4.6%, 9.8%, and 29.7%, 10.7%, 12.6%, respectively. Furthermore, 3D geometrical data, including surface area $S$, volume $V$, and sphericity $\varphi$ of single cells, were successfully obtained. This demonstrated that the developed microscope system can efficiently and accurately capture and characterize the true 3D geometry of cells, emphasizing its scientific value.

**Keywords:** cell observation instrument, 3D geometric information, fruit single cell, dual-viewpoint, orthogonal observation
**DOI:** 10.25165/j.ijabe.20251803.9581

**Citation:** Qiang H L, Li B L, Li Z G, Tchuenbou-Magaia F, Wei B Y, Liu Y D. Novel technique for measuring the 3D geometric size of fruit cells. Int J Agric & Biol Eng, 2025; 18(3): 257–264.

## 1 Introduction

Fruits exhibit intricate hierarchical structures which affect their properties, including morphology and texture. At the macro-scale, they are composed of various tissue types, each comprising highly organized arrangements of cells[1]. Studies have shown that cell size affects important traits such as size and texture of apple, banana, and cherry fruit[2-4]. Cell dimensions play a crucial role in the variation of apple texture, with larger cells being linked to increased juiciness[5,6]. Fruit single cells exhibit a diverse range of shapes[7,8]. Due to these shape irregularities[9], two-dimensional (2D) images captured using conventional microscopes are unable to characterize their true geometry. Consequently, exploring a two-view orthogonal observation method to obtain precise 3D geometrical information of individual fruit cells is of great scientific value. This approach will enhance the characterization of cell structures and provide deeper insights into the complexities of fruit texture and quality.

The emergence of the microscope greatly accelerated human exploration of the microscopic world, providing a bridge between the known macrocosm and the unknown microcosm[10]. Previous studies on the observation of morphological dimensions of single cells of fruits can be categorized into two approaches: single-view biomicroscopic and multi-view biomicroscopic characterization. For instance, scanning electron microscopy (SEM) has been employed to examine apple tissues, revealing that the epidermis functions as the boundary tissue between the apple and its environment. This epidermis consists of two layers of small skin cells. Furthermore, the morphology of the apple cells varies from rectangular or triangular to thin or flattened shape[11]. The micro- and macro-structural changes during the osmotic dehydration of apple slices were investigated using light microscopy (LM) and environmental scanning electron microscopy (ESEM), and it was found that the tissues of the fresh samples showed pronounced cellular interstitials, with both cells and interstitial spaces loosely arranged in a reticulated pattern that was inhomogeneous and anisotropic[12]. In contrast, multi-view biomicroscopic characterization provides more comprehensive information. For example, a high strain rate micro compression test setup using dual-view imaging revealed that tomato cells were elongated and irregularly shaped, with heights ranging from 230-540 $\mu$m, averaging 372±7 $\mu$m, and height ratios ranging from 0.56-1.14, with a mean ratio of 0.81[13]. X-ray microcomputed tomography revealed a significant difference in the size and shape distribution between the dermal and thin-walled cells of pear[14].

In summary, although microscopes have been extensively used to observe cellular structures and analyze the geometric and morphological information of fruit single cells, conventional microscopes merely provide observations from a single viewpoint, resulting in 2D images that do not capture the thickness direction of fruit cells or reveal the hidden areas between cells[15]. Therefore, the goal of this study was to develop a microscope system for imaging

**Received date:** 2024-11-29 **Accepted date:** 2025-04-13
**Biographies:** **Hongli Qiang**, MSc. candidate, research interest: agricultural engineering, Email: qhl1364208185@163.com; **Baolong Li**, MSc. candidate, research interest: agricultural engineering, Email: 2734901540@qq.com; **Fideline Tchuenbou-Magaia**, PhD, Reader, research interest: agricultural engineering, Email: F.Tchuenbou-Magaia@wlv.ac.uk; **Boyuan Wei**, Senior engineer, research interest: mechanical engineering, Email: 18945069411@163.com; **Yande Liu**, PhD, Professor, research interest: agricultural engineering, Email: jxliuyd@163.com.

***Corresponding author: Zhiguo Li**, Professor, research interest: agricultural engineering.College of Mechanical and Electronic Engineering, Northwest A&F University, Yangling 712100, Shaanxi, China. E-mail: lizhiguo0821@163.com.

single fruit cells from both orthogonal and elevation angles to accurately characterize their 3D geometry while improving measurement efficiency.

## 2 Materials and methods

### 2.1 Development of a 3D cell observation instrument

Figure 1 depicts the concept for the design. The biomicroscope is designed to provide detailed information on the shape contours of fruit single cells along the *x*- and *z*-axes of the 3D Cartesian coordinate system. Two light sources were strategically positioned: one in front of the sample chamber along the *x*-axis and another on top along the *z*-axis. Filters were placed in front of both light sources to minimize the impact of color differences[16-18]. The photomicrographic observation system utilized an infinity flat-field compound achromatic objective lens, paired with the light source on the *x*-axis, to observe front view images of single cells of fruits. Additionally, a second photomicrographic observation system was utilized, which also employed an infinity flat-field compound achromatic objective lens. This system, in conjunction with the light source oriented in the *z*-axis direction on a glass trough, was used to observe bottom images of single cells of the fruit.

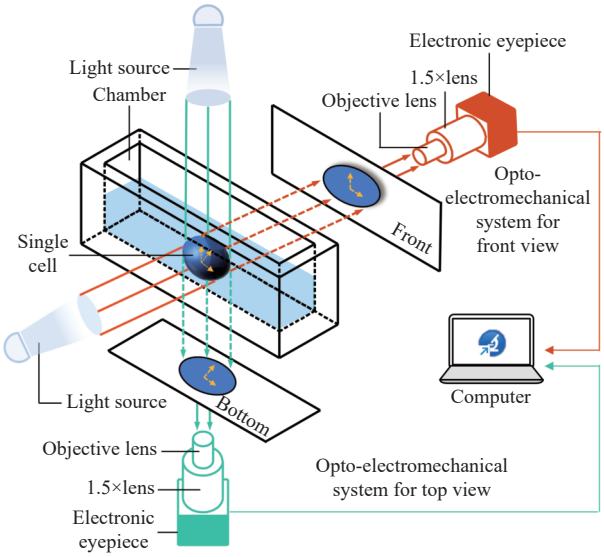


Figure 1 Conceptual design for the 3D cell observation instrument

#### 2.1.1 Design concept of the microscope system for 3D cell observation

1) Design of the observation system for improving imaging resolution

The 3D cell observation instrument provides contour information of individual fruit cells from two orthogonal perspectives: the front and the bottom. Achieving high clarity in single-cell imaging is of paramount importance. This investigation focused on optimizing both the choice of objective lenses and the design of the sample chamber to enhance image clarity. The numerical aperture is a critical parameter that reflects the light-accepting ability of the microscope lens and directly influences image sharpness. The numerical aperture is proportional to the refractive index of the medium and the sine of the half-angle of the light cone. A higher numerical aperture value indicates stronger light collection by the microscope lens, resulting in a clearer image[19,20]. To enhance image sharpness, the aim was to maximize the half-angle of the light cone while maintaining a constant medium. Unlike ordinary objective lenses, the infinity-corrected flat-field compound achromatic objective lens can achieve a light cone half-angle approaching 90°, thereby maximizing the numerical aperture and producing the sharpest possible image. The sample chamber serves as the medium for cell observations, with its shape and texture significantly influencing image clarity. The chamber was designed in a rectangular shape to minimize shape distortion commonly introduced by arc-like structures during observation[21]. Additionally, the wider rectangular shape, compared to a square shape, effectively reduces the imaging focal length, thereby extending the working range of the 3D cell observation instrument. Under the influence of gravity, the cells in the sample chamber sink to the bottom surface of the rectangular body, necessitating the objective lens to observe cells at the junction of the sidewalls and the bottom surface. To minimize the traces at the junctions of the sample chamber, a specialized gluing technique was employed to precisely bond the high-purity quartz glass pieces. This approach ensures a clear and traceless outline of the observed cells, thereby enhancing overall imaging quality.

2) Designing for improving observation efficiency

Fruit cells are inherently 3D structures with varying shapes and sizes, as opposed to flat, 2D structures[22]. Therefore, it is necessary to observe fruit single cells from two orthogonal view directions to accurately obtain 3D dimensional information such as length, width, thickness, etc. To sustain the single cell activity, the isolated fruit single cells were placed in a sample chamber containing a 0.9% NaCl solution (length×width×height: 17 mm×5 mm×6 mm, thickness 1 mm). The cell observation instrument, as depicted in Figure 1, primarily consists of a light source system and two separate, orthogonal photoelectric microscopic viewing systems.

During the observation of single cells, the paths of the two photomicrographic observation systems may intersect on different planes, potentially affecting the precise localization of individual cells. To resolve this issue, the focal points of both observation systems were aligned on a single plane. The *y*-axis direction of the photomicrographic observation system observing the front view image and the *x*- and *y*-axis directions of the system observing the bottom view image were fixed. The 3D geometry of a single cell of a fruit is accurately observed through the relative movement of the sample chamber along the *x*- and *y*-axis directions. Consequently, this configuration allows for precise localization of cells in both views, while also simplifying the structure of the device and improving its observation efficiency. Finally, electronic eyepieces were installed on both photomicrographic observation systems, enabling the dual-view images of single cells to be transmitted to the computer software, which was utilized to obtain high-resolution single-cell images. Then, the upper computer software was utilized to measure the dimension of the acquired front and bottom images of single cells, thereby providing the 3D geometrical dimensions of fruit single cells.

#### 2.1.2 Hardware integration of the 3D cell observation instrument

The microscope system developed in this study for cell characterization, as depicted in Figure 2, primarily consists of a light source system and two independent, orthogonal photomicrographic observation systems designed to fulfill the aforementioned requirements. The light source system features a 3W high brightness LED, two types of filters (blue and green), a light switch knob, and a light adjustment disk. This system controls both the illumination and brightness, creating optimal lighting conditions for the experiment. Color casts are less noticeable on tests when lights are used in tandem with filters. The photoelectric microscopic observation system for observing fruit single cell frontal views mainly includes: electronic eyepiece with 10-million-

pixel resolution CMOS image sensor (PH100-3A41L-A; Phoenix Optics Co., Ltd., China), 1.5× coated restoration lens (Phoenix Optics Co., Ltd., China), 2×, 4×, 10× infinite flat field apochromatic objective lens (Phoenix Optics Co., Ltd., China), and three-axis moving platform with an accuracy of 0.01 mm (*x*-axis focusing direction moving range: ±6.5 mm, *z*-axis moving range: ±5 mm, moving accuracy is 0.01 mm) (Shenzhen Huike Pneumatic Precision Machinery Co., Ltd., China). The photoelectric microscopic observation system used to observe the bottom views of fruit single cells mainly includes: electronic eyepiece with 10-million-pixel resolution CMOS image sensor (PH100-3A41L-A; Phoenix Optics Co., Ltd., China), 1.5× coated restoration lens (Phoenix Optics Co., Ltd., China), 2×, 4×, 10× infinite flat field apochromatic objective lens, and a three-axis moving platform with an accuracy of 0.01 mm (*z*-axis focusing direction moving range: ±5 mm, moving accuracy is 0.01 mm). The main elements of the stage are the sample chamber (length×width×height: 17 mm×5 mm×6 mm, thickness 1 mm), a three-axis moving platform with an accuracy of 0.01 mm (*x*-axis moving range: ±6.5 mm, *y*-axis moving range: ±5 mm, moving accuracy of 0.01 mm), and the support module. Front and bottom view calibrators (Hazen Technology Co., Ltd., China) are used to calibrate the actual magnification of the cell. To calibrate the actual magnification of the front and bottom views of the microscope, the calibrator is placed in the stage position by the fit between the slots. The rotary lever conversion device, consisting of a rotary handle and a rotary button, facilitates the adjustment of the differential head of the three-axis moving platform. The microscope system is enclosed in a protective cover that is securely attached to the base plate, providing protection against dust and damage. It has tiny openings that allow the rotating handle to come out of action, making the operation easier for the user.

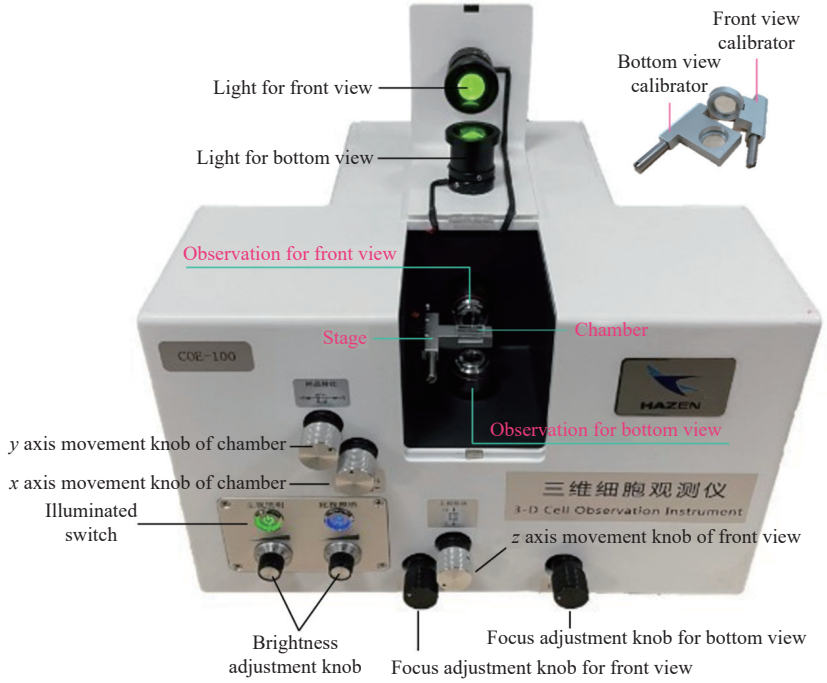


Figure 2 Microscope system for 3D cell morphological characterization

2.1.3 Software development for the novel microscope system

A computer software was created to support the developed microscope system. It is an easy-to-use image measurement and analysis software. The software development flowchart is outlined in Figure 3a. The camera module, measurement module, and image processing module were developed using different technologies, including Visual Studio software, the Windows Form foundation, and the C# programming language, all based on the Open CV sharp library. Since the cell viewer has two photomicrographic observation systems, a multi-threading technique was implemented to synchronize the display of front and bottom view images within a single window, as illustrated in Figure 3b.

The primary features of the computer software include image flipping, geometric measuring, calibration, brightness and contrast adjustment, and image saving. The image flipping function allows for more accurate descriptions of the various cell states and simplifies subsequent image processing. The developed software was used to measure the front view image and the bottom view image of the fruit single cell, respectively, providing the length and width of each image. Since the two images obtained are orthogonal, a comparative analysis allowed for the determination of the 3D geometry of the fruit single cell, including its length, width, and thickness.

2.1.4 Performance calibration of 3D cell observation instrument

The quality of the cell image is determined by the performance of the cell observation instrument. This section details the measurement and assessment of key performance indicators to ensure high imaging quality. These indicators include total mass, overall size, objective magnification, electronic eyepiece pixels, electronic eyepiece magnification, total magnification, working distance, focal length, focal length accuracy, multi-hole diameter, resolution, field area, accuracy of the three-axis moving platform, and the observation range of cell observation instrument.

The total mass and overall size of the cell observation instrument were measured, respectively, using an electronic industrial scale with an accuracy of 10 g (measuring range: 200 kg, Delixi Electric Co., Ltd., China) and a stainless-steel ruler with an accuracy of 1 mm (measuring range: 50 cm, Guangzhou Xintian Tools Co., Ltd., China). The electronic eyepiece magnification was determined by dividing the diagonal size of the computer-generated

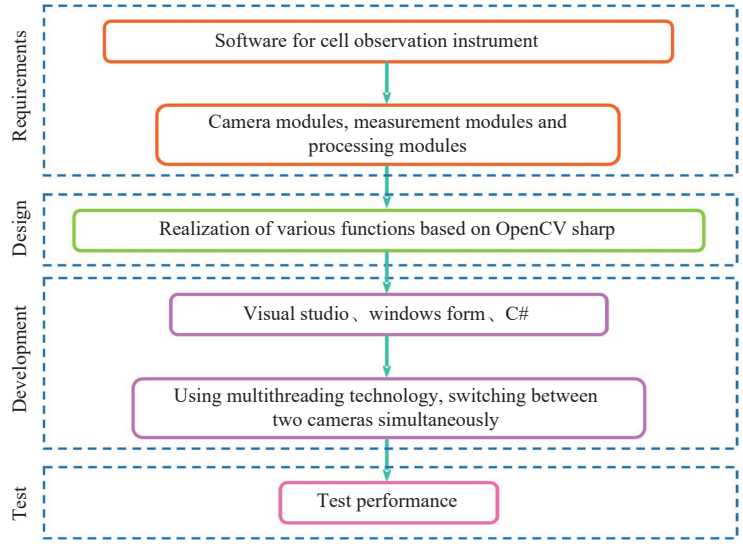


a. Computerized observation software development flowchart

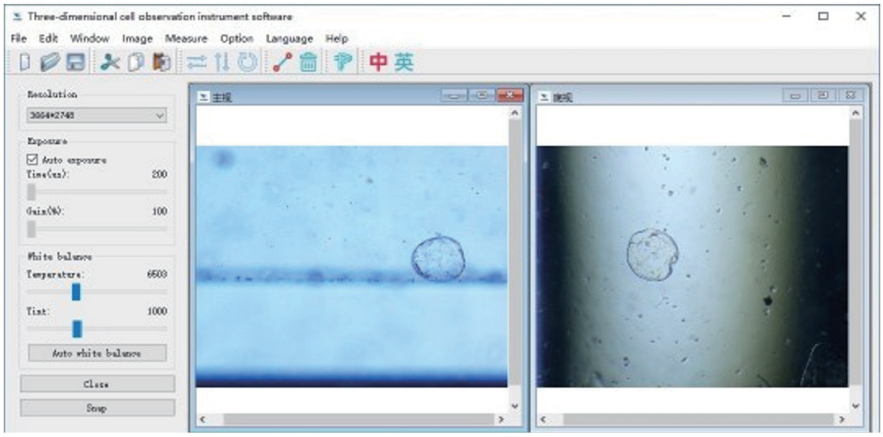


b. Observation software interface diagram

Figure 3 Flowchart of the cell observation software development

picture's field of view by the diagonal size of the electronic eyepiece's image sensor. To ensure that the geometrical size of the observed cells is consistent with the actual size of the cells, scales (measuring range 1 cm, 1DIV=0.1 mm) were used to calibrate the front and bottom views. The images were calibrated by means of a ruler so that the measured cell sizes reflect their actual dimensions. The calibration scales were imaged by the two photomicrographic observation systems, respectively. The overall magnification of the view was calculated as the difference between the size of the ruler on the computer screen and the actual size of the ruler being observed. This method was used to determine the overall magnification of the photoelectric microscopic observation system. Once the total magnification of the developed microscope was established, the area observed by the front and bottom view photoelectric micro-observation systems was computed to determine the field of view area. The observation range of the photoelectric micro-observation system is primarily determined by the adjustment range of the three-axis moving platform. When a clear frontal view of the cell was visible, the photomicrographic observation equipment was adjusted to monitor the single fruit cell. The working distance of the front view photoelectric micro-observation system is defined as the vertical distance between the surface of the objective lens and the single fruit cell. The photoelectric microscopic observation system of the bottom image of the fruit single cell was adjusted to achieve a clear bottom cell image. The working distance of the bottom image photoelectric microscopic observation system is the vertical distance between the surface of the objective lens and the fruit single cell. The focal length of the photoelectric micro-observation system was measured as the distance from the center of the lens to its focal point. Equation (1) was used to determine the numerical aperture NA of the photomicrographic observation system[8,19,20]. Equation (2) was used to determine the resolution $D$ of the cell viewer[8].

$$\mathrm{NA} = n \times \sin\alpha \tag{1}$$

$$D = \frac{0.61 \times \lambda}{\mathrm{NA}} \tag{2}$$

where, NA is the numerical aperture of the achromatic objective lens; $n$ is the refractive index of the optical medium between objective lens and single cell; $\alpha$ is the aperture angle of the objective lens, (°); $D$ is the resolution of an opto-electromechanical microscopic observation system, nm; $\lambda$ is the wavelength of the illumination source, nm.

### 2.2 Determination of the 3D geometry information of fruit single cells

Ten "Hongyan" strawberries and ten fresh, ripe "Provence" tomatoes were acquired in May 2023 at Yangling Agricultural High-Tech Industrial Demonstration Zone of China. As illustrated in Figure 4, the fruit is cut into two parts by the biological blade in the direction of the center axis. Figure 4a depicts the division of the tomato into the mesocarp, septal, and central regions[23], whereas

Figure 4b shows the division of the strawberry into the external and interior tissue parts[24,25].

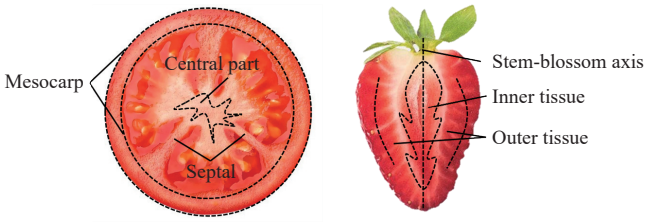


a. Fruit cross-section of a tomato b. Fruit longitudinal-section of a strawberry

Figure 4 Tomato and strawberry fruit cross section

Since the primary components of interest are the mesocarp of the tomato and the external tissue of the strawberry, cells were isolated from these tissues for further characterization. A biological blade was used to cut the fruit test portion into a square sample measuring 20 mm×5 mm. The square sample was gently brushed with a test tube brush (medium, Beekman Biotechnology Co., Ltd., China) numerous times diagonally over a clean dish containing 20 mL of water. This process dislodged the cells, allowing them to adhere to the side wall of the dish. The cells adhered to the side wall of the Petri dish were then carefully transferred into clean water using a 200 uL pipette with a 5×49 mm pipette tip attached to a 3 mL plastic dropper head. The target cells were isolated to ensure minimal contamination, and complete single cells were selected for further testing.

Undamaged cells were transferred to a sample chamber (length×width×height: 17 mm×5 mm×6 mm, thickness 1 mm) containing a 0.9% NaCl solution at a depth of 1 mm for observation. When examining the front view of a single fruit cell, the photomicrographic observation system was configured to illuminate the front-view light source while dimming the bottom-view light source. Conversely, the bottom-view light source was illuminated while the front-view light source was dimmed when observing the cell's bottom view. The front and bottom views of the single fruit cells were recorded using the computer software. Finally, the software was then used to measure the 3D geometry of the two recorded photos. The cell volume was calculated based on the ellipsoidal shape of the observed tomato and strawberry cells. From the front and bottom view images, the largest diameter of the single cell was identified as its main axis diameter (diameter 1), aligned with the length direction. The minor axis diameter (diameter 2) in the thickness direction was taken as the diameter of the equatorial section perpendicular to the main axis in the same perspective. In another view, the minor axis diameter (diameter 3) representing the breadth direction was considered the diameter orthogonal to both the main axis (diameter 1) and the minor axis (diameter 2). Equation (3) was used to determine the geometric mean diameter of the single cell[8,9,25], Equation (4) to determine its sphericity[8,9,26], Equation (5) to determine its surface area[8,25,26], and Equation (6) to determine its volume[8,27].

$$GMD = (D_1 \times D_2 \times D_3)^{1/3} \tag{3}$$

$$\varphi = \frac{GMD}{D_1} \tag{4}$$

$$S = \pi \times (D_1 \times D_2 \times D_3)^{2/3} \tag{5}$$

$$V = \frac{1}{6} \times \pi \times D_1 \times D_2 \times D_3 \tag{6}$$

where, $GMD$ is the geometric mean diameter of the fruit single cell, $\mu$m; $D_1$ is the maximum maximal diameter of a single cell as seen from the front and bottom, $\mu$m; $D_2$ is the equatorial diameter in the same perspective perpendicular to $D_1$, $\mu$m; $D_3$ is the diameters orthogonal to $D_1$ and $D_2$ in the other view, respectively, $\mu$m; $\varphi$ is the sphericity of the fruit single cell; $S$ is the surface area of the fruit single cell, $\mu m^2$; $V$ is the volume of the fruit single cell, $\mu m^3$.

## 3 Results and discussion

### 3.1 Performance parameters of the developed microscope

Table 1 presents the performance indices of the 3D cell observation instrument. The cell observation instrument's weight was determined to be 7.16 kg, and its entire dimension was 345×300×215 mm. The use of a 4-infinite flat-field compound achromatic objective lens enabled clear visualization of the front view of individual cells. The photomicrographic observation system captured both the front and bottom images of single cells with a working distance of 20 mm, a focal length of 50 mm, and a focal length accuracy of 0.01 mm. The 3D cell observation instrument provided a clear view of the calibration scale, with a resolution calculated to be up to 2.5 $\mu$m. Higher resolution lenses revealed more detailed cell structures, allowing for more precise measurements. Calibration tests determined the total magnification of the instrument to be 80× for both front and bottom views, with a calculated field of view of 5.19 mm² for both perspectives. The microscope's observation range was found to be 1300 $mm^3$, facilitated by the three-axis moving stage, which has an accuracy of 0.01 mm. The $x$-axis has a travel range of ±6.5 mm, while the $y$- and $z$-axes each have a range of ±5 mm, with fine adjustment precision in all directions at 0.01 mm. Given that fruit single cells range in size from tens to hundreds of micrometers[28-31], this 3D cell observation instrument is highly suitable for accurately analyzing the 3D geometry of fruit single cells.

**Table 1 Performance parameters of the 3D cell observation instrument**

| Parameter | Value | Parameter | Value |
|---|---|---|---|
| Mass | 7.16 kg | Size | 345×300×215 $mm^3$ |
| Objective magnification | 2×; 4×; 10× | Numerical aperture | 0.15 |
| Eyepiece pixel | 1000 W | Electronic eyepiece magnification | 30× |
| Front view magnification | 80× | Bottom view magnification | 80× |
| Objective lens working distance | 20 mm | Focal length | 50 mm |
| Focal length accuracy | 0.01 mm | Resolution | 2.5 $\mu$m |
| Front view area | 5.19 $mm^2$ | Bottom view area | 5.19 $mm^2$ |
| Three-axis moving platform accuracy | 0.01 mm | Observation range | 1300 $mm^3$ |

### 3.2 3D analysis of single cells of fruits

The 3D cell observation instrument developed in 2.1 was used to investigate the tomato pericarp cells, with the resulting front and bottom views shown in Figure 5. The outlines of the pericarp cells in the four tomatoes (A, B, C, and D) are clearly visible in Figure 5, exhibiting uniformity and smoothness in cell structure. Figure 6 depicts the front and bottom views of the exterior tissue cells of strawberries, as observed with the same 3D cell observation instrument. Figure 6 vividly depicts the cell outlines in the four strawberry fruits' (A, B, C, and D) exterior tissues, showing irregular shapes. The 3D cell observation instrument effectively highlights broken cells, as seen in Figure 5d and Figure 6d. Notably, it was impossible to determine whether the cells were broken or not

if only a single viewpoint was used, emphasizing the significance of the 3D cell observation instrument. From the illustration, it can be inferred that the morphology of the cells varies significantly, with differences in morphological dimensions both within the same region of a single fruit and between cells from different fruits. In particular, tomato pericarp cells exhibit distinct morphologies, with cells farther from the exocarp being larger and more irregular in size, while those closer to the exocarp are smaller[32,33]. The morphology of observed cells was in accordance with these reports, suggesting the reliability of the developed instrument.

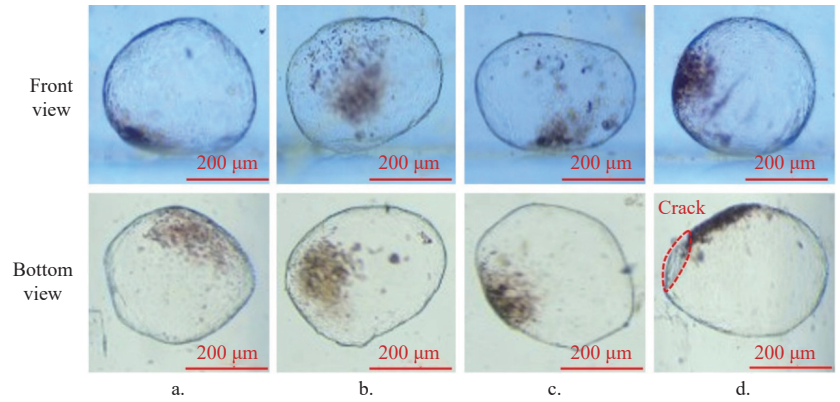


Note: a. tomato mesocarp single cell A; b. tomato mesocarp single cell B; c. tomato mesocarp single cell C; d. tomato mesocarp single cell D.

Figure 5 Front and bottom view images of single cells of the tomato mesocarp

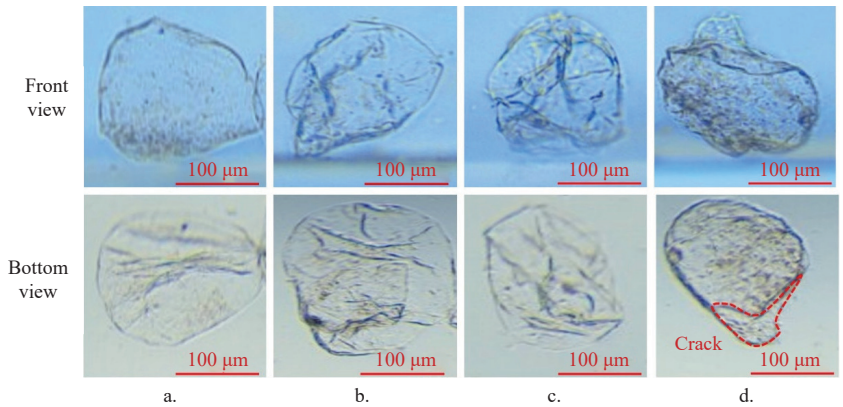


Note: a. strawberry external tissue cell A; b. strawberry external tissue cell B; c. strawberry external tissue cell C; d. strawberry external tissue cell D.

Figure 6 Front and bottom view images of strawberry external tissue cells

Table 2 displays the geometrical dimensions of the tomato peel cells and the cells of the strawberry external tissues as determined by measurement of the 3D cell observation instrument and derivation of Equations (3)-(6). Utilizing the cell observation instrument and computer software, data on the length, width, and thickness of a single cell were obtained. These geometric dimensions were then used to calculate the geometric mean diameter, sphericity, surface area, and volume of a single cell according to the empirical formulas in 2.2. The length $D_1$ of tomato pericarp cells ranged from 402.16-532.49 $\mu$m, thickness $D_2$ from 306.39-441.23 $\mu$m, width $D_3$ from 223.64-485.36 $\mu$m, and the geometric mean diameter $GMD$ from 314.29-466.07 $\mu$m. The surface area $S$ ranged from $4.1\times10^5$-$6.8\times10^5$ $\mu m^2$, with the volume $V$ ranging from $1.6\times10^7$-$5.3\times10^7$ $\mu m^3$, and the sphericity $\varphi$ from 0.69-0.91. Strawberry external tissue cells had a length $D_1$ ranging from 293.53-364.03 $\mu$m, thickness $D_2$ from 153.71-286.95 $\mu$m, width $D_3$ from 110.29-292.028 $\mu$m, geometrical mean diameter $GMD$ from 224.62-289.57 $\mu$m, surface area $S$ from $1.6\times10^5$-$2.6\times10^5$ $\mu m^2$, volume $V$ from $0.6\times10^7$-$1.3\times10^7$ $\mu m^3$, and sphericity $\varphi$ ranging from 0.68-0.84. As indicated in Table 2, the strawberry external tissue cells are smaller in length, width, and thickness compared to the tomato pericarp cells. Additionally, the strawberry external tissue cells have a smaller surface area and volume, though no significant difference in sphericity is observed. When tomato mesocarp cells were examined under a biomicroscope, the majority of the cells had oval shapes[34]. The 2D measurements of the individual cells in both fruits were consistent with earlier findings[7,35,36]. The data ranges of geometric mean diameter $GMD$, surface area $S$, volume $V$, and sphericity $\varphi$ of tomatoes and strawberries obtained in this study are

**Table 2 Geometric parameters of single cells of the pericarp region in tomato and single cells of the external tissue of strawberry (mean±standard deviation, $n$=20)**

| 2D/3D scene | Geometric parameter | Tomato pericarp cells | Strawberry external tissue cells |
|---|---|---|---|
| 2D geometric parameters | $D_1$, $\mu$m | 474.27±51.62 | 331.46±19.79 |
| | $D_2$, $\mu$m | 382.95±101.64 | 228.20±35.25 |
| | $D_3$, $\mu$m | 361.93±57.36 | 223.40±41.49 |
| 3D geometric parameters | $GMD$, $\mu$m | 401.34±67.35 | 255.55±27.65 |
| | $\varphi$ | 0.84±0.09 | 0.77±0.06 |
| | $S$($\times10^5$), $\mu m^2$ | 5.20±1.68 | 2.07±0.45 |
| | $V$($\times10^7$), $\mu m^3$ | 3.67±1.68 | 0.91±0.29 |

Note: $D_1$ is the maximum maximal diameter of a single cell as seen from the front and bottom, $\mu$m; $D_2$ is the equatorial diameter in the same perspective perpendicular to $D_1$, $\mu$m; $D_3$ is the diameters orthogonal to $D_1$ and $D_2$ in the other view, respectively, $\mu$m; $GMD$ is the geometric mean diameter of fruit single cell; $\varphi$ is the sphericity of fruit single cell; $S$ is the surface area of fruit single cell; $V$ is the volume of fruit single cell.

consistent with the data ranges of 3D geometric information of tomatoes and strawberries observed by previous researchers[7,13,28]. These results further validate the accuracy and reliability of the developed computer software and the 3D cell observation instrument.

The length $D_1$, thickness $D_2$, and width $D_3$ represent the 2D diameter measurements of the cell, while the mean geometric diameter *GMD* represents the 3D diameter measurement of the cell. As shown in Table 2, the 3D diameter data obtained using the 3D cell observation instrument developed in this study differs significantly from the 2D diameter data acquired through a single-view biomicroscope. Specifically, the discrepancies between the length $D_1$, thickness $D_2$, and width $D_3$ compared to the geometric mean diameter *GMD* for the pericarp cells in tomato were 18.18%, 4.6%, and 9.8%, respectively. For strawberry external tissue cells, the discrepancies were 29.7%, 10.7%, and 12.6%, respectively. The aforementioned differences show that for a 3D cell morphology, the 2D size of the cell observed through the single-view angle biomicroscope cannot accurately characterize the 3D geometric properties of the cell. An inevitable gap between the 3D geometric information collected and the 2D geometric information of individual fruit cells has been demonstrated[8], which is consistent with the findings of this study. In previous research, a 2D image of a single apple cell was captured using a light microscope. The 2D image was then converted to a binary image, and the grayscale image of the cropped single cell was manually segmented into a binary image. From the binary image, the characteristics of the cell were determined, including its diameter, area, roundness, aspect ratio, and roughness[37]. However, there was a significant deviation between the cell diameters obtained from these 2D images and the real apple cell diameters, leading to inaccuracies in the measured values for area, roundness, aspect ratio, and roughness, ultimately affecting the reliability of the test results. In another study, histological examinations of microscopic cross sections of transgenic tomato pericarp cells were conducted using a computerized section scanner to compare cell sizes across various tomato varieties[38]. Discrepancies were identified, illustrating that determining cell size based solely on the diameter observed in cross sections does not account for the full 3D structure of the cells, and also does not accurately represent the level of cell size across different tomato varieties. In contrast, the 3D cell observation instrument developed in this study provides accurate 3D geometric information, facilitating a more precise characterization of cell morphology. This approach addresses the limitations of traditional 2D microscopy, ensuring that the true geometric properties of cells are captured and analyzed comprehensively.

## 4 Conclusions

This study presents a novel dual-view orthogonal approach for observing and characterizing the 3D geometrical properties of single fruit cells. By utilizing the newly developed 3D cell observation instrument, front and bottom views of single fruit cells were captured and analyzed using computer software, enabling precise measurements of key 3D geometric parameters such as length, width, and thickness. The dual-view biomicroscope consists of a light source system with two orthogonal, independent photomicrographic observation systems at 80×magnification. The photomicrographic observation system can capture front and bottom views, and the microscope's resolution can reach 2.5 $\mu$m. Cells with diameters from 2.5 $\mu$m to 1000 $\mu$m can be clearly observed. The performance of this system was evaluated using ripe strawberries and tomatoes. The results demonstrate that the instrument effectively captures clear, detailed outlines of single cells, revealing variations in cell shape and size. Additionally, the computer software enables precise determination of the 3D geometric size of single cells. Notably, the 3D geometric sizes of strawberry external tissue cells are smaller than those of tomato pericarp cells. This highlights the system's capability to accurately describe the 3D geometry of cells, which cannot be accomplished accurately with traditional 2D biomicroscopes. Moreover, cells are prone to damage when they are affected by disease or external forces, leading to alterations in cell size. The developed 3D cell observation instrument is particularly advantageous in this regard, as it determines whether a cell is diseased by measuring the size of the cell, and presents attractive potential in a wide range of applications, not only for plant cells but also for animal cells.

## Acknowledgements

This work was supported by the International Cooperation Key Plan of Shaanxi Province (Grant No. 2022KWZ-12) and the National Key Research and Development Program of China (Grant No. 2025YFE0108600). This work was also supported by the Faculty of Science and Engineering of the University of Wolverhampton Visiting Researcher Grant and EU Horizon 2020 MSCA RISE Project ReACTIVE Too, Grant Agreement No. 871163.

## [References]

[1] Li Z G, Thomas C. Quantitative evaluation of mechanical damage to fresh fruits. Trends in Food Science & Technology, 2014; 35(2): 138–150.

[2] Jullien A, Munier-Jolain N G, Malézieux E, Chillet M, Ney B. Effect of pulp cell number and assimilate availability on dry matter accumulation rate in a banana fruit. Annals of Botany, 2001; 88(2): 321–330.

[3] Olmstead J W, Iezzoni A F, Whiting M D. Genotypic differences in sweet cherry fruit size are primarily a function of cell number. Journal of the American Society for Horticultural Science, 2007; 132(5): 697–703.

[4] McAtee P A, Hallett L C, Johnston J W, Schaffer R J. A rapid method of fruit cell isolation for cell size and shape measurements. Plant Methods, 2009; 5(1): 5.

[5] Bertin N, Gautier H, Roche C. Number of cells in tomato fruit depending on fruit position and source-sink balance during plant development. Plant Growth Regulation, 2002; 36(2): 105–112.

[6] Mann H, Bedford D, Luby J, Vickers Z, Tong C. Relationship of instrumental and sensory texture measurements of fresh and stored apples to cell number and size. HortScience, 2005; 40(6): 1815–1820.

[7] Liu Z G, Li Z G, Yue T L, Diels E, Yang Y G. Differences in the cell morphology and microfracture behaviour of tomato fruit (*Solanum lycopersicum L.*) tissues during ripening. Postharvest Biology and Technology, 2020; 164: 111182.

[8] Zhang M S, Yang J, Wang Y H, Li Z G, Tchuenbou-Magaia F. A new method for reconstructing the 3D shape of single cells in fruit. Food Research International, 2022; 162: 112017.

[9] Li Z G, Zhang Z B, Thomas C. Viscoelastic-plastic behavior of single tomato mesocarp cells in high speed compression-holding tests. Innovative Food Science & Emerging Technologies, 2016; 34: 44–50.

[10] Wang Y, Zhang X S, Xu J, Sun X Y, Zhao X L, Li H S, et al. The development of microscopic imaging technology and its application in micro- and nanotechnology. Frontiers in Chiemistry, 2022; 10: 931169.

[11] Allan-Wojtas P, Sanford K A, McRae K B, Wojtas P A, Carbyn S. An integrated microstructural and sensory approach to describe apple texture. Journal of the American Society for Horticultural Science, 2003; 128(3): 381–390.

[12] Nieto A B, Salvatori D M, Castro M A, Alzamora S M. Structural changes in apple tissue during glucose and sucrose osmotic dehydration: shrinkage, porosity, density and microscopic features. Journal of Food Engineering, 2004; 61(2): 269–278.

[13] Wang C X, Pritchard J, Thomas C R. Investigation of the mechanics of single tomato fruit cells. Journal of Texture Studies, 2006; 37(5): 597–606.

[14] Mebatsion H K, Verboven P, Jancsok P T, Ho Q T, Verlinden B E, Nicolaï B M. Modeling 3D fruit tissue microstructure using a novel ellipsoid tessellation algorithm. CMES-Computer Modeling in Engineering & Sciences, 2008; 29(3): 137–150.
[15] Zhou L L, Cai M J, Tong T, Wang H D. Progress in the correlative atomic force microscopy and optical microscopy. Sensors, 2017; 17(4): 938.
[16] Anjam K. A method of dynamic chromatic aberration correction in low-voltage scanning electron microscopes. Ultramicroscopy, 2005; 103(4): 255–260.
[17] Fu M L, Fan T C, Lu C X, Lai J S, Zhang W Q, Antonov E, et al. Light filters influence on the chromaticity for Fresnel microprisms. Optik, 2020; 201: 163484.
[18] Liu Z X. Third-rank chromatic aberrations of electron lenses. Ultramicroscopy, 2018; 185: 27–31.
[19] Arash D, Vahid A. Dielectric microspheres enhance microscopy resolution mainly due to increasing the effective numerical aperture. Light-Science Applicationgs, 2023; 12: 22.
[20] Zhang C L. Methods and instruments for the measurement of numerical aperture for microscope objective lens: A mini review. Review of Science Instruments, 2022; 93(11): 113705.
[21] Ji P, Lee S S, Im Y E, Choi Y. Determination of geometry-induced positional distortion of ultrafast laser-inscribed circuits in a cylindrical optical fiber. Optics Letters, 2019; 44(3): 610–613.
[22] Gray J D, Kolesik P, Høj P B, Coombe B G. Confocal measurement of the three‐dimensional size and shape of plant parenchyma cells in a developing fruit tissue. Plant Journal, 1999; 19(2): 229–236.
[23] Li Z G, Li P P, Yang H L, Liu J Z, Xu Y F. Mechanical properties of tomato exocarp, mesocarp and locular gel tissues. Journal of Food Engineering, 2012; 111(1): 82–91.
[24] An X, Liu H J, Fadiji T, Li Z G, Dimitrovski D. Prediction of the temperature sensitivity of strawberry drop damage using dynamic finite element method. Postharvest Biology and Technology, 2022; 190: 111939.
[25] An X, Li Z G, Zude-Sasse M, Tchuenbou-Magaia F, Yang Y G. Characterization of textural failure mechanics of strawberry fruit. Journal of Food Engineering, 2020; 282: 110016.
[26] Han X W, An X, Fadiji T, Li Z G, Khojastehpour M. Textural thermo-mechanical properties of sweet cherry for post-harvest damage analysis. Journal of Texture Studies, 2022; 53(4): 453–464.
[27] Singh S S, Abdullah S, Pradhan R C, Mishra S. Physical, chemical, textural, and thermal properties of cashew apple fruit. Journal of Food Process Engineering, 2019; 42(5): e1394.
[28] An X, Li Z G, Wegner G, Zude-Sasse M. Effect of cell size distribution on mechanical properties of strawberry fruit tissue. Food Research International, 2023; 169: 112787.
[29] Zhao F F, Zhang J J, Weng L, Li M, Wang Q H, Xiao H. Fruit size control by a zinc finger protein regulating pericarp cell size in tomato. Molecular Horticulture, 2021; 1: 6.
[30] Mauxion J P, Chevalier C, Gonzalez N. Complex cellular and molecular events determining fruit size. Trends in Plant Science, 2021; 26(10): 1023–1038.
[31] Zhao X, Muhammad N, Zhao Z X, Yin K L, Liu Z G, Wang L X, et al. Molecular regulation of fruit size in horticultural plants: A review. Scientia Horticulturae, 2021; 288: 110353.
[32] Legland D, Guillon F, Kiêu K, Bouchet B, Devaux M F. Stereological estimation of cell wall density of DR12 tomato mutant using three-dimensional confocal imaging. Annals of Botany, 2010; 105(2): 265–276.
[33] Legland D, Devaux M F, Bouchet B, Guillon F, Lahaye M. Cartography of cell morphology in tomato pericarp at the fruit scale. Journal of Microscopy, 2012; 247(1): 78–93.
[34] Zdunek A, Kurenda A. Determination of the elastic properties of tomato fruit cells with an atomic force microscope. Sensors, 2013; 13(9): 12175–12191.
[35] Azzi L, Deluche C, Gévaudant F, Frangne N, Delmas F, Hernould M, et al. Fruit growth-related genes in tomato. Journal of Experimental Botany, 2015; 66(4): 1075–1086.
[36] Vallarino J G, de Abreu e Lima F, Soria C, Tong H, Pott D M, Willmitzer L, et al. Genetic diversity of strawberry germplasm using metabolomic biomarkers. Science Reports, 2018; 8: 14386.
[37] Cárdenas-Pérez S, Chanona-Pérez J J, Méndez-Méndez J V, Calderón-Domínguez G, López-Santiago R, Arzate-Vázquez I. Nanoindentation study on apple tissue and isolated cells by atomic force microscopy, image and fractal analysis. Innovative Food Science & Emerging Technologies, 2016; 34: 234–242.
[38] Gan L J, Song M Y, Wang X C, Yang N, Li H, Liu X X, et al. Cytokinins is involved in regulation of tomato pericarp thickness and fruit size. Hortic Research, 2022; 9: uhab041.